ChemSusChem

Review
doi.org/10.1002/cssc.202300729

Chemistry Europe
European Chemical Societies Publishing

www.chemsuschem.org

Catalytic Graphitization of Biocarbon for Lithium-Ion Anodes: A Minireview

Lillian Lower[+],[a] Shaikat Chandra Dey[+],[b] Trevor Vook,[a] Mark Nimlos,[c] Sunkyu Park,[b] and William Joe Sagues*[a]

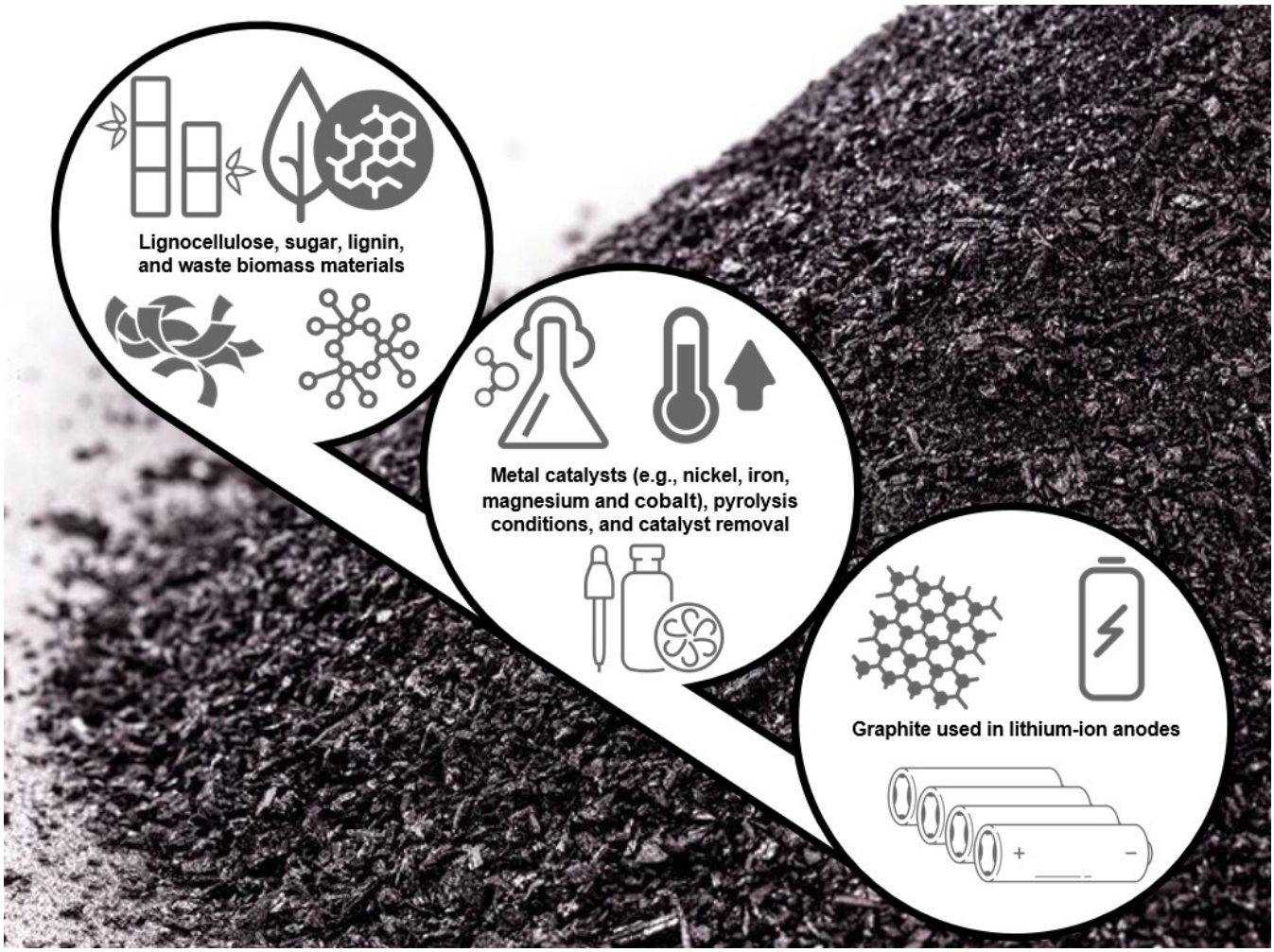

The demand for electrochemical energy storage is increasing rapidly due to a combination of decreasing costs in renewable electricity, governmental policies promoting electrification, and a desire by the public to decrease CO_2 emissions. Lithium-ion batteries are the leading form of electrochemical energy storage for electric vehicles and the electrical grid. Lithium-ion cell anodes are mostly made of graphite, which is derived from geographically constrained, non-renewable resources using energy-intensive and highly polluting processes. Thus, there is a desire to innovate technologies that utilize abundant, affordable, and renewable carbonaceous materials for the sustainable production of graphite anodes under relatively mild process conditions. This review highlights novel attempts to realize the aforementioned benefits through innovative technologies that convert biocarbon resources, including lignocellulose, into high quality graphite for use in lithium-ion anodes.

1. Introduction

Lithium-ion batteries are the leading form of electrochemical energy storage for electric vehicles and the electrical grid.[1–6] Graphite anode material accounts for approximately 15–30% of lithium-ion cell mass and costs $8–$13 per kilogram; graphite prior to downstream purification and shaping varies in cost, but is generally considerably lower than final anode product.[7] Graphite's ABA stacking of graphene sheets allow for effective intercalation and de-intercalation of lithium ions when charging and discharging a cell, respectively, as shown in Figure 1. In addition, the chemical inertness, structural stability, and relatively low weight of graphite make it suitable for use in lithium-ion cell anodes. By 2050, the use of graphite in energy storage capacities is expected to increase by 500% if climate change is limited to an increase in two degrees celcius.[8]

There are two types of graphite used in industrial applications: mineral and synthetic. Graphite anodes used in lithium-ion batteries are often comprised of both mineral and synthetic graphite.[7,10–12] Processing mineral graphite for lithium-ion anode applications often involves the use of hydrofluoric acid (HF) for purification, which can be detrimental to human health and the environment due to its highly corrosive nature.[4,13–15] Synthetic graphite offers advantages over mineral graphite including more consistent quality and higher electrochemical performance.[13] Synthetic graphite is usually produced by using high aromatic, low sulfur fossil carbon resources, such as fluid catalytic cracking (FCC) slurry oil, via delayed coking at 475–530 °C to form needle coke, which is then calcined at 1100–1500 °C and graphitized at 2000–3000 °C for more than 7 days.[7,16] The emissions associated with synthetic graphite production are significant, reaching as high as 20 kg CO_2e per kg graphite.[8] Thus, there is a need for new technologies that utilize abundant, affordable, and renewable carbonaceous materials for the sustainable production of graphite anodes under relatively mild process conditions.

Renewable biocarbon resources, including lignocellulose, hold the potential to be sustainable, non-toxic, domestic, and relatively low-cost feedstocks for carbonaceous energy storage materials, including graphite anodes.[17] However, unlike certain fossil carbon resources, biocarbon resources generally do not graphitize when treated at elevated temperatures, but rather carbonize into disordered carbon.[18–20] Carbonized biocarbon materials typically do show some evidence of graphite structure, but the crystal size and extent of graphitization are usually small, thus making them inferior to commercial Li-ion anode materials.[19,21,22] Innovative approaches, using metal catalysts or chemical activators, must be taken to convert disordered biocarbon into graphitic carbon with relatively high electrochemical performance as anode material. Recently, catalytic graphitization methods have been developed and published, demonstrating the ability to produce high quality graphite from biomass, which is now referred to as "biographite". For the first time, this review highlights recent innovations in catalytic graphitization of biomass resources for application as Li-ion battery anode material. In this review, biographite is defined as biomass-derived carbon materials with crystalline graphite features of varying extents and sizes. Relative to other reviews on biomass carbon materials, this review narrowly

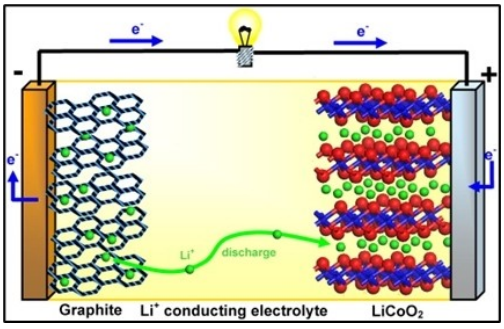

Figure 1. Schematic of a lithium-ion electrochemical cell with a graphite anode and lithium cobalt oxide cathode.[9] Reproduced from ref. [9] Copyright (2008), with permission from Wiley-VCH.

[a] *L. Lower,[+] T. Vook, Prof. Dr. W. J. Sagues*
Department of Biological and Agricultural Engineering
North Carolina State University
3110 Faucette Dr., Raleigh, NC 27695 (USA)
E-mail: wjsagues@ncsu.edu

[b] *S. C. Dey,[+] Prof. Dr. S. Park*
Department of Forest Biomaterials
North Carolina State University
2820 Faucette Dr., Raleigh, NC 27695 (USA)

[c] *Dr. M. Nimlos*
Materials, Chemical, and Computational Science Directorate
National Renewable Energy Laboratory
15013 Denver West Parkway, Golden, CO 80401 (USA)

[+] *These authors contributed equally to this work.*

focuses on the limited number of studies that involve lithium-ion battery applications. Specifically, process parameters are highlighted including biomass feedstock type, catalyst type, catalyst loading, graphitization temperature, heating rate, hold time, and resultant graphite crystallite size. In addition, critical electrochemical performance metrics are highlighted including specific capacity, capacity loss, and coulombic efficiency. Graphite needs to meet optimal size, shape, and purity requirements for consideration for lithium-ion anode material. These requirements are, briefly, approximately 12–20 μm sized spherical agglomerates for optimal balance between coulombic losses, packing efficiencies, reversible capacity, and surface area, and a purity of at least 99.9% carbon.[10,23] Physical characteristics, such as shape, size, and purity of graphitic carbon materials are necessary qualities for initial consideration for lithium-ion applications, but they are not always fully represented in academic studies. Using physiochemical properties alone as the qualifying metrics for biographite anode materials is not sufficient, and future studies should apply and assess the biographite materials in actual electrochemical cells.Therefore, this review has focused more on lab-scale electrochemical performance as an indicator for graphite quality, and included physical characteristics where pertinent. Current commercial lithium-ion cells with graphite anodes achieve capacities of ~350 mAh g^{-1} with less than 1% loss over 100 cycles and initial coulombic efficiencies $>$ 90%, and thus these represent targets for biographite innovators.[22,24]

2. Traditional Methods of Graphite Production

2.1. Graphite Production from Mineralized Carbon

Mineral graphite is extracted from the earth via mining operations in particular locations and processed via several resource-intensive operations, as shown in Figure 2.[4,15,18,24] In 2021, China was responsible for 79% of global graphite production, with North America producing 1.2%, thereby highlighting the geographically constrained nature of mineral graphite production.[25,26] Mineral graphite concentrates contain non-carbon impurities including carbonate and silicate minerals, which often require hydrofluoric acid to reach the desired purity. Current industry practices require battery-grade mineral graphite to be milled and shaped into a spherical form prior to purification.[10] Hydrofluoric acid purification is costly, detrimental to the environment, and a public health risk. Lithium-ion battery manufacturers are beginning to favor the use of synthetic graphite over mineral graphite given the geographic constraints, expensive processing, and use of harsh chemicals for purification of mineral graphite, as well as the relatively high quality and performance of synthetic graphite.

2.2. Traditional Graphite Production from Fossil Carbon

Currently, approximately 50% of graphite used in lithium-ion anodes is synthetically produced from fossil carbon resources, such as petroleum-derived FCC slurry oil.[13,15] Notably, the use of synthetic graphite in lithium-ion anodes is increasing and expected to reach 70% by 2030 due to the higher quality and reliability relative to mineral graphite.[13] As shown in Figure 3, the generation of petroleum-derived

Lillian Lower received her M.S. degree in Biological and Agricultural Engineering from North Carolina State University in 2023. She is currently a Ph.D. student in the Biocarbon Utilization and Sequestration (BUS) Lab at North Carolina State University and is advised by Dr. Joe Sagues. Her research focuses on catalytic graphitization of biomass materials for use in lithium-ion battery applications.

Shaikat Chandra Dey is a Ph.D. student in the Department of Forest Biomaterials at North Carolina State University, working under the supervision of Professor Sunkyu Park. His research focuses on iron-catalyzed conversion of pyrolysis oil into biographite for lithium-ion anode applications. He obtained his M.S. Degree in Applied Chemistry and Chemical Engineering from the University of Dhaka, Bangladesh, in 2016. Before joining the Ph.D. program in 2021, he served as a full-time faculty (Assistant Professor) in the same department at the University of Dhaka.

Dr. Sagues is the Principal Investigator of the Biocarbon Utilization & Sequestration (BUS) Lab in the Biological & Agricultural Engineering Department at North Carolina State University. He has experience in research, development, and demonstration of innovative bioprocessing technologies at corporations, universities, and national labs. The BUS Lab takes an integrated approach to innovate technologies that utilize and sequester biogenic carbon in valuable products, including biographite anodes for lithium-ion batteries.

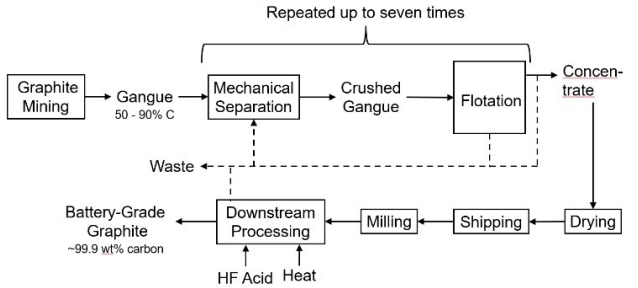

Figure 2. Simplified process flow diagram of battery-grade graphite production from mineral graphite where downstream processing includes necessary purification, milling, shaping, and coating.

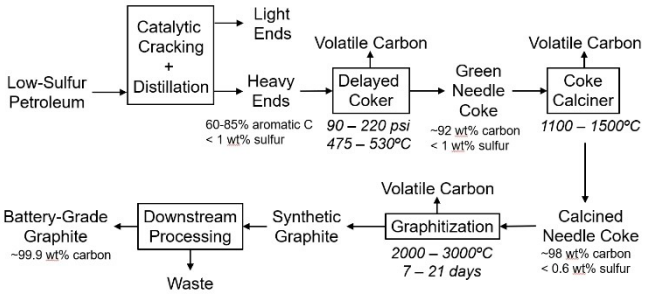

Figure 3. Simplified process flow diagram of battery-grade graphite production from petroleum where the final step, downstream processing, includes necessary purification, milling, shaping, and coating.

needle coke and subsequent graphitization is the most common method for producing synthetic graphite. High molecular weight polyaromatic hydrocarbons with fused rings, such as anthracene and acenaphtalene, are of the ideal structure to partially graphitize into needle coke.[16] During delayed coking and calcining, polyaromatics progressively fuse to form a material of turbostratic structure, as shown in Figure 4. During graphitization, the turbostratic carbon becomes more organized to ultimately form highly ordered, crystalline graphite.

There are four main impediments to petroleum-derived needle coke's future as a carbon precursor for battery-grade graphite: 1) geographic constraints, 2) capital intensive operations, 3) policy barriers, and 4) energy requirements. As shown in Figure 3, the process of converting heavy ends from low-sulfur petroleum refining to battery-grade graphite involves multiple, highly energy-intensive operations. The composition of heavy ends must be high in aromatic carbon content and low in sulfur content, which is only possible from high quality, low impurity sweet crudes. Thus, suitable heavy ends for needle coke production are geographically constrained to regions with particular crude composition. Finally, the energy required to convert petroleum to synthetic graphite is immense, resulting in up to 20 kg CO_2e per kg graphite.[8] As nations move away from processes that involve fossil carbon combustion, alternative sources of energy to provide the high quantity of high temperature heat needed for synthetic graphite production may be cost prohibitive.

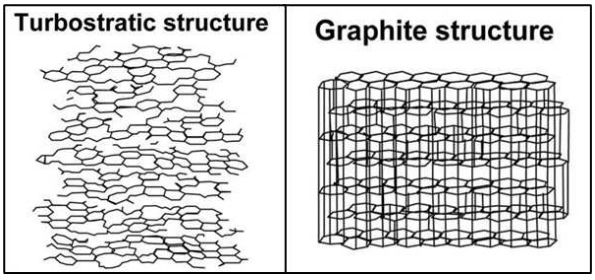

Figure 4. Molecular structures of turbostratic carbon (left) and graphitic carbon (right).[27] Reproduced from ref. [27] Copyright (2012), with permission from Soil Science Society of America.

2.3. Novel Graphite Production from Fossil Carbon

As a possible way to reduce energy requirements, attempts have been made to prepare graphite from fossil carbon materials at relatively lower temperatures by the use of suitable graphitization catalysts. Yang et al. utilized a magnesium catalyst to convert anthracite, or hard coal, to graphite-containing carbon material for applications in lithium and potassium ion batteries.[28] 1.5 g anthracite was mixed with 1.5 g magnesium and graphitized at 600, 800, and 1100 °C for 2 hours (heating rate of 5 °C min^{-1}). Electrochemical performance in lithium-ion batteries was best from the 1100 °C anode material with a reversible capacity of approximately 326 mAh g^{-1} at 100 mA g^{-1} for 100 cycles and nearly 100% capacity retained from the second cycle. The coulombic efficiency was initially 36%. Electrochemical performance when used in potassium ion batteries was best from the 800 °C graphite with a reversible capacity of 141 mAh g^{-1} with an initial coulombic efficiency of 32%.[28] Along with magnesium, iron-based catalysts have been used to successfully produce graphite at lower temperatures. Nugroho et al. prepared graphite from petroleum coke via pyrolysis at 1300 °C (3 h with 10 °C min^{-1} heating rate) with iron catalysts (Fe and Fe_2O_3).[29] Petroleum coke was dry-mixed with catalysts to a loading of 40% iron. The resulting graphite crystallite sizes were 13.4 nm, 18 nm, and 17.7 nm for the no catalyst, iron catalyst, and Fe_2O_3 catalyst sample groups, respectively. It was concluded that the larger crystallite sizes resulting from the catalyzed methods would demonstrate better lithium-ion insertion and de-insertion performance, so only the iron-catalyzed graphites were used for electrochemical performance testing in coin-cells. Both samples performed similarly with a reversible capacity of 100 mAh g^{-1} at 0.25 C, capacity retention of 80% at 10 C, and coulobmic efficiency of 80%.[29] Zhao et al. also used an iron-based catalyst to catalytically graphitize ball-milled carbon at loading rates of 10, 20, 30, and 40 wt% and at temperatures of 200, 1100, and 2000 °C (3 hour hold time with 5 °C min^{-1} heating).[30] Graphite crystallite size increased with temperature for each loading rate with the largest L_c sizes of 56.9 nm and 57.3 nm for the samples with 10 wt% and

40 wt% catalyst loading treated at 2000 °C, respectively. Electrochemical performance of the 40 wt% iron loading treated at 2000 °C resembled that of commercial graphite with a reversible capacity of 360 mAh g^{-1} at 0.2 C, initial coulombic efficiency of 85%, and low capacity loss after the first cycle.[30] This process produced anode material at lower temperatures than typically required for synthetic graphite production (3000 °C), which may lead to potentially lower production costs.[30] Although the number of studies on catalytic conversion of fossil carbon to anode materials is relatively low, the aforementioned evidence indicates there is potential for impactful technology advancements. However, interest in catalytic conversion of renewable and more sustainable feedstocks, such as biocarbon, to anode materials is growing faster than that of fossil carbon resources.

2.4. Graphite Production from Biocarbon

Technologies that carbonize biomass into biocarbon products such as biochar and activated carbon have progressed significantly over the past two decades.[31–33] Graphitization of biomass has historically not been of significant interest due to inherent structural limitations. Glucose, lignin, cellulose, lignocellulose, and other biomaterials are classified as non-graphitizing materials that generate char products when processed at elevated temperatures (1000–3000 °C), whereas particular heavy ends of petroleum refining are considered graphitizing materials that generate soft carbon products rich in graphite crystallites.[16] The lack of fused aromatic rings and the abundance of carbon-oxygen and sp3 hybridized carbon-carbon bonds in biomass lead to disordered char material; during carbonization, the sp3 hybridization of carbon atoms in biomass allows for free rotation during thermal cleavage, resulting in random and disorder upon condensation and structural rearrangement.[16] Thus, overall, material scientists and engineers have not viewed biocarbon-derived graphite, or biographite, as a potential replacement to mineral- or fossil carbon-derived graphite.

3. Graphite Production via Catalytic Graphitization

Certain non-graphitizing materials, including lignocellulose, will graphitize in the presence of metal catalysts during pyrolysis at relatively low temperatures (<1500 °C), see Table 1. This phenomena was first discovered in the steel manufacturing process wherein impurities skimmed from molten iron in the basic oxygen furnace, collectively referred to as "kish", were found to contain high levels of graphite among other impurities including calcium, magnesium, sulfur, and silica.[34] During smelting, iron in the presence of carbon will form molten eutectic iron-carbon alloys (~1200 °C) that precipitate graphite when annealed. Steel manufacturing processes are typically optimized to minimize

Table 1. Electrochemical performance data from selected studies that catalytically graphitized biocarbon for use as anode material in lithium-ion batteries.

Feedstock	Catalyst Type	Specific Capacity	Retention Efficiency	Initial Coulombic Efficiency	Ref.
Softwood	Reduced iron powder	340, 300, 245, 120, 40, and 15 mAh g^{-1} at 0.1, 0.5, 1, 2, 4, and 8 C	89% over 100 cycles at 0.5 C	84%	[39]
Medium Density Fiberboard	Iron Chloride	307 mAh g^{-1} at 0.1 C	90% after 200 cycles at 1 C	64%	[40]
Medium Density Fiberboard	$Ni(NO_3)_2$	204 mAh g^{-1} at 37.2 mA g^{-1}	35% at 3720 mA g^{-1} from 37.2 mA g^{-1}, 97% after 200 cycles at 372 mA g^{-1}	27%	[41]
Hardwood Sawdust	Iron powder	353 mAh g^{-1} after 100 cycles at C/2	99% over 100 cycles at C/2	84%	[23]
Hardwood Sawdust	Iron powder	357 mAh g^{-1} after 100 cycles at C/2	>99% after 100 cycles at C/2	92.3%	[42]
Bacterial Cellulose	Ferrous Acetate	529 mAh g^{-1} after 100 cycles at 0.2 C	81% over first 20 cycles at 0.2 C	55%	[43]
Chitosan	$Fe(NO_3)_3$	423 mAh g^{-1} after 100 cycles at 0.1 Ag^{-1}	85% after 200 cycles at 2 Ag^{-1}	45%	[44]
Algae	$Ni(NO_3)_2$	1006.4 mAh g^{-1} at 0.1 Ag^{-1}, 278.2 mAh g^{-1} at 5 Ag^{-1}, and 520 mAh g^{-1} at 1 Ag^{-1} after 500 cycles	92.3% over 500 cycles at 1 Ag^{-1}	66.5%	[45]

graphite formation in kish. There has been some interest in separating graphite from kish as a value-added coproduct, however, the high levels of impurities, particularly silica, make processing and purification costly.[34] Nickel, cobalt, and magnesium are additional metals that have demonstrated, similar to iron, the ability to incorporate, or dissolve, carbon, creating a metal-carbide that precipitates graphite in the molten phase (1200–1400 °C).[35–37] Metal-catalyzed graphite grows in the vertical c-axis to a greater extent than mineral graphite, which typically favors the lateral α-axis.[26,27,38] Thus, the morphologies of metal catalyzed graphite typically consist of crystallites with high dimension ratios of vertical stacking (L_c) to horizontal expansion (L_a) (Figure 5), making them suitable for lithium-ion intercalation and de-intercalation.[30] Unlike most high-value graphite applications, lithium-ion anodes do not require large flake graphite morphologies with extensive L_a dimensions, hence why synthetic graphite performs well.[13] Thus, metal-catalyzed graphitization is a promising pathway to provide sustainable graphite anode materials for the growing lithium-ion industry. In general, there are two reported methods of doping biomass with metal catalyst: wet and dry methods. Wet methods involve soaking the biomass in a liquid solution wherein the solubilized metal salts are distributed within the pores of the biomass. Upon drying, some metal ions are retained within the biomass and subsequently catalyze graphitization at elevated temperatures. Dry methods are simpler than wet methods and involve mixing metals, typically in reduced form (not salts), with biomass. Notably, dry methods appear to provide graphite of similar, if not higher, quality than wet methods and do so in a relatively simple and less costly manner. However, the field of research is still relatively young and more time is needed to reach consensus around the advantages and disadvantages of wet and dry methods.

3.1. Catalytic Graphitization of Lignocellulosic Feedstocks

The most abundant complex natural biopolymer on earth is lignocellulose, which consists of lignin, cellulose, and hemicellulose. In lignocellulosic biomass, the non-carbohydrate phenolic polymer (lignin) strongly binds to carbohydrate polymers (cellulose and hemicellulose) and strengthens and hardens plant cell walls. Lignocellulosic biomass has been extensively researched to produce renewable fuels as well as numerous valuable industrial chemicals due to its widespread availability and low cost.[46,47] Recently, efforts have been made to develop electrode-grade carbon materials from lignocellulose through catalytic graphitization. Banek et al. developed a two-step biomass graphitization process using an iron catalyst with the first step involving pyrolysis of lignocellulosic biocarbon and iron catalyst pellets at 600 °C (heating of 30 °C min^{-1} and held for 30 minutes) to create biochar, and the second step involved CO_2 laser ablation of the biochar-iron pellets to generate highly crystalline (L_c: 32 nm, L_a: 77 nm) battery-grade graphite with a final purity of 99.95 %.[23] The loading of iron prior to the initial heat treatment was 2 g per 6 g biomass (33 wt %). Following laser ablation, acid washing and microwave digestion were employed to remove the catalyst. Overall, this two-step process converted 95.7 % of the biochar into graphite. The resultant graphite had a crystallite size of 32 nm. Electrochemical performance testing of the graphite resulted in a reversible capacity of 353 mAh g^{-1} at 0.5 C over 100 cycles, with a retention efficiency of 99 % (Figure 6). The initial coulombic efficiency of the anode material was 84 %, which could likely be improved by lowering the surface area of the graphite. Banek et al.'s process successfully converted a variety of biocarbon precursors to graphite, thereby demonstrating the ability to be feedstock agnostic.[23] Banek et al. repeated their two-step process in a second study in which lignocellulosic materials were mixed with an iron catalyst,

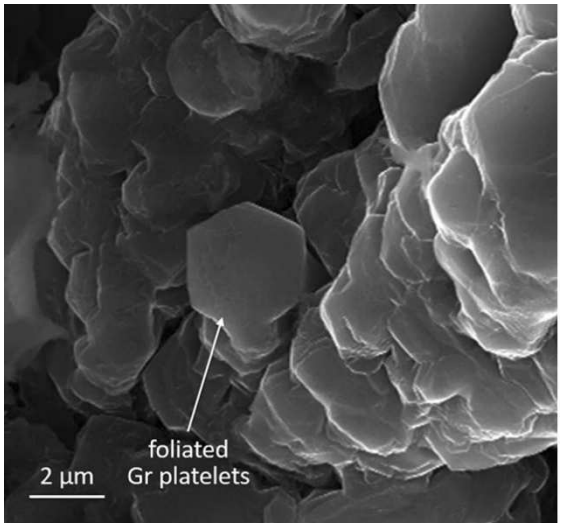

Figure 5. Vertical foliated growth of graphite platelets from molten iron-carbon.[25] Reproduced from ref. [25] Copyright (2016), with permission from Wiley-VCH.

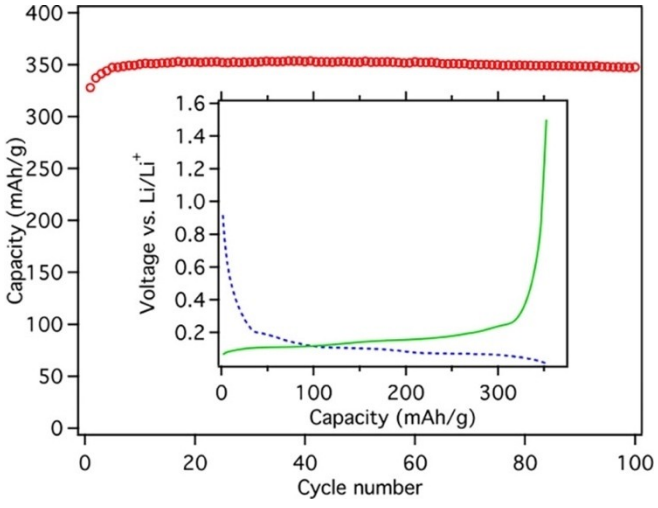

Figure 6. Electrochemical performance data of biographite materials used as anode material in lithium-ion cells.[23] Reproduced from ref. [23] Copyright (2018), with permission from American Chemical Society. Further permissions related to the material excerpted should be directed to the ACS.

pressed into pellets, pyrolyzed, and irradiated by a laser.[42] Alternatively to the aforementioned study, this process required a diode laser, not a CO_2 laser. Following laser treatment, the graphitized material was ground and purified to remove the iron catalyst following the previous methods. The graphite material performed well in lithium-ion battery testing with a reversible capacity of 357 mAh g^{-1} over 100 cycles at 0.5 C with no capacity loss. The initial coulombic efficiency was 92.3%.[42] This study achieved a significant advancement in biographite production by demonstrating a direct synthesis of graphite agglomerates of the desired size for downstream processing, thereby potentially by-passing expensive and wasteful shaping operations. The use of laser ablation worked well in both studies at the lab-scale, but is not common in industrial scale pyrolysis or graphitization operations.[23] An alternative route for the conversion of lignocellulosic biomass to lithium-ion battery anode material was described by Sagues et al. Various biomass feedstocks (Figures 7 and 8) were processed via iron-catalyzed graphitization to produce high-quality graphite anode material.[39] Reduced iron powder was used as the catalyst with loading of 30 wt% and annealing was performed at 1200 °C with a heating rate of 10 °C min^{-1} and hold time of 1 hour. X-ray diffraction (XRD) was used to qualify the crystallinity of the various biographite samples in comparison to commercial graphite (Figure 8). XRD diffractograms provide both qualitative and quantitative assessments of graphite quality. As shown in Figure 8, commercial graphite has characteristic peaks at 2-theta degrees of 26°, 42°, 44°, and 55°. Biochar and other disordered biocarbon materials typically have a broad, low intensity peak at 26° and little to no peak definition at the other characteristic degrees, indicating non-graphitic structure. As shown in Figure 8, iron-catalyzed graphitization of biomass results in highly defined, narrow peaks at all characteristic degrees, thereby indicating large crystal dimensions. Softwood-derived graphite crystallite size was approximately 25 nm. Electrochemical performance testing with the softwood-derived biographite showed strong performance in a lithium-ion cell with reversible capacities of 340 and 300 mAh g^{-1} at 0.1 and 0.5 C, respectively, retention efficiency of 89% over 100 cycles and an initial coulombic efficiency of 84%. Hardwood biomass feedstock was also used as a catalytic graphitization feedstock and produced slightly lower quality graphite relative to softwood, so it was not evaluated for electrochemical performance.[39]

Unlike the studies conducted by Banek et al. and Sagues et al., which detailed dry-mixing powdered catalyst with biomass, Gomez-Martin et al. prepared graphite anodes from lignocellulosic material soaked, or wet-mixed, with an iron catalyst.[40] Commercial medium density fiberboard (MDF) was soaked in a 1 M iron chloride solution before carbonization. Pyrolysis was conducted at temperatures of 850–2000 °C with heating rates of 1 °C min^{-1} to 500 °C and 5 °C min^{-1} to the maximum temperature before being held for 30 minutes. TEM imaging of the iron chloride within the resultant graphite shell are shown in Figure 9. Graphite crystallite size generally increased with temperatures with sizes of 9.3, 9.8, 30.2, 45, 41.7, and 46.8 nm for pyrolysis temperatures of 850, 1000, 1200, 1400, 1600, and 2000 °C, respectively. Electrochemical performance analysis was conducted using the anode material produced at 2000 °C. The specific capacity was found to be 307 mAh g^{-1} at 0.1 C with capacity retention greater than 90% after 200 cycles at 1 C. The initial coulombic efficiency was 64%.[40] Gomez-Martin et al. conducted a subsequent study to evaluate the effects of different metal-catalysts on the graphitization of MDF, using a nickel catalyst to transform recycled MDF into

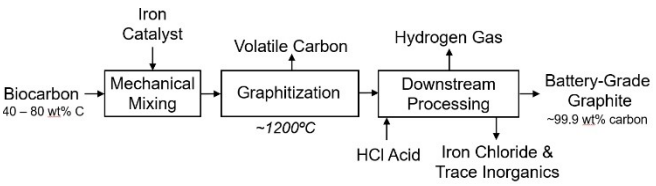

Figure 7. Process flow diagram of catalyzed graphitization of biomass where the final step, downstream processing, involves necessary purification, milling, shaping and coating.

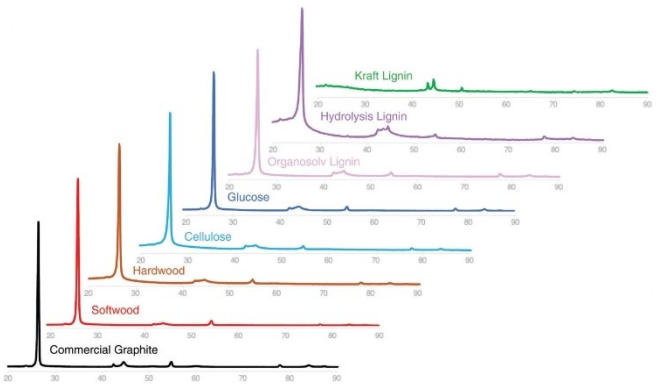

Figure 8. X-ray diffractograms of biographite materials generated from iron-catalyzed graphitization.[39] 2-theta degree of diffraction and intensity shown in x- and y-axes, respectively. Reproduced from ref. [39] Copyright (2020), with permission from Royal Society of Chemistry.

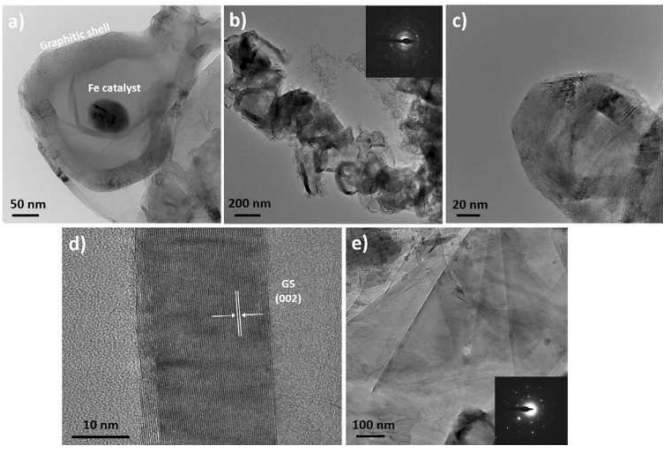

Figure 9. Catalytically graphitized biomass samples before (a) and after catalyst (iron) removal (b–e).[40] Reproduced from ref. [40] Copyright (2018), with permission from Wiley-VCH.

graphene-like porous nanosheets.[41] MDF samples were dried, cut, and immersed in a 3 M solution of nickel II nitrate before being pyrolyzed at two different temperature conditions: 300 and 1000 °C (both with a hold time of 30 minutes and a ramping rate of 5 °C min^{-1}). From XRD and Raman spectroscopy analysis it was concluded that the 1000 °C pyrolysis treatment produced higher quality graphite, and only this sample group was evaluated for performance in lithium-ion battery cell testing. The anode material demonstrated a reversible capacity of 204 mAh g^{-1} at 37.2 mA g^{-1}. Capacity retention was approximately 97% after 200 cycles at 372 mA g^{-1}. Initial coulombic efficiency was 27%.[41] Lignocellulosic by-products and waste materials from processing systems have been investigated for possible biographite precursors to increase overall circularity and sustainable reuse of materials. Destyorini et al. conducted wet mixing to utilize a waste product from coconut processing.[48] Several combinations of chemical activation and nickel catalysts were investigated to graphitize coconut coir, the rough hair removed from coconut shells. Raw coir was carbonized, ground, and immersed in a mixed solution of KOH and nickel (II) chloride hexahydrate (ANi) at ratios of 1 : 1 carbon to KOH, 1 : 1.2 carbon to ANi, and 1 : 1 : 1.2 carbon to KOH to ANi. Graphitization was performed at 1200 °C for 3 hours with a heating rate of 5 °C min^{-1}. The best treatment according to electrochemical performance was the combined activator-catalyst group with the highest specific capacity of 397.6 mAh g^{-1} and capacity retention efficiency of 87.35% at 0.5 C current density for 30 cycles. The initial coulombic efficiency was 72.11%.[48]

While studies discussed herein have focused on lignocellulosic biomass graphitization because of the feedstock's low-cost availability, biomass feedstocks that are predominantly composed of cellulose have also been considered for catalytic graphitization. Wu et al. performed catalytic graphitization of degreasing cotton using iron (III) acetylacetone as the catalyst.[49] Cotton was chosen because it is a low-cost graphite precursor with scalable applications. Degreasing cotton (3 g) was immersed in 20 mL dimethylformamide solution with 10 mmol iron (III) acetylacetone before catalytic graphitization at 650 °C for 3 hours. The composite material had a crystallite size of 35 nm. Electrochemical testing resulted in reversible capacities of 1070 mAh g^{-1} after 430 cycles at 0.2 C, 950 mAh g^{-1} after 100 cycles at 1 C and 850 mAh g^{-1} after 200 cycles at 2 C. The coulombic efficiency of the anode material was initially 72% and 99% after 430 cycles.[49] Bacterial cellulose produced via microbial fermentation has been proven to be a viable candidate for lithium-ion battery anode material.[43] Illa et al. reported a method for carbon nanofiber production from bacterial cellulose via iron-catalyzed graphitization. Ferrous acetate was incorporated into the bacterial cellulose at 0.1 wt% before graphitization at 900 and 1800 °C (with ramping of 5 °C min^{-1} and a hold time of 1 hour). The resulting material was described as having predominantly hard carbon features with turbostratic stacking and some graphitic crystallites. The graphite crystallite sizes for the non-catalyzed samples were 0.82 nm and 1.37 nm for the 900 °C and 1800 °C temperature groups. Use of the iron catalyst increased graphite crystallite size to 0.85 nm and 4.32 for the 900 °C and 1800 °C temperature treatments. The catalytically derived nanofibers produced at 900 °C displayed the best electrochemical performance with a reversible capacity of 529 mAh g^{-1} after 100 cycles at 0.2 C and 19% capacity loss after 20 cycles. The coulombic efficiency of the anode material was 55% from the first cycles, and 99% at the final cycles.[43] While the aforementioned graphitization of degreasing cotton and bacterial cellulose produced remarkably high reversible capacities, the low initial coulombic efficiencies of 72% and 55%, respectively, reflect potential impurities in the anode material and shorter battery lifetimes.[50]

Although limited in number, the aforementioned studies have successfully demonstrated catalytic graphitization of lignocellulosic materials at relatively low temperatures. Gaps in research exist around the optimal catalyst loadings and effects of ash components in lignocellulosic feedstocks. Inorganic ash comprises 3–10 wt% of many lignocellulosic materials and contains metals including Si, Al, Mn, and Fe, among others.[51] Future studies should explore the use of lignocellulose materials high in magnesium and iron since these are proven catalysts for biographite production. In addition, there is intriguing potential for production of high performing lithium-ion anode materials from lignocellulose materials rich in silicon since the electron storage capacity of silicon is 800% greater than graphite.[52] Industry reports indicate commercial lithium-ion cells under development for electric vehicles are doped with small quantities of silicon due to the significant increase in energy density achieved.[53] Researchers should assess the ability for naturally occurring silicon in lignocellulosic materials to enhance the energy storage of biographite anodes. Finally, the number of studies on catalytic graphitization of lignocellulose biomass for lithium-ion anode application are very small, and thus activity needs to increase rapidly if such technologies are to become commercially relevant in the near future.

3.2. Catalytic Graphitization of Carbohydrate Feedstocks

In addition to lignocellulosic materials, studies have demonstrated the catalytic conversion of carbohydrates to biographite to increase knowledge of fundamental mechanisms. Carbohydrates, including simple sugars such as glucose and xylose, can be used as model compounds for more complex biopolymers including cellulose and hemicellulose. The use of pure carbohydrates allows researchers to increase quality control and better understand the mechanisms at play. There is some interest in using carbohydrates for commercial production, but the feasibility is relatively low given that carbohydrates are quite expensive and this approach would directly compete with food production. Glucose and sucrose are the two carbohydrates that have been investigated the most for graphite anode production.[41–45] Sagues et al. determined that iron-catalyzed graphitization of glucose

produces the largest graphite crystallites when heated rapidly, as compared to slowly.[39] However, the degree of graphitization was highest with relatively slow heating of glucose in the presence of iron. Upon heating, most simple carbohydrates melt prior carbonizing and graphitizing. During the melting process, it's possible that metal catalyst particles diffuse to allow for more uniform distribution throughout the substrate, which would ultimately increase the degree of graphitization. A slower rate of heating allows more time for the catalyst particles to diffuse during the melting process thereby increasing the degree of graphitization. Furthermore, the onset temperature for glucose graphitization was found to be ~600 °C, considerably less than that of lignocellulose. Sagues at al. observed that the yield of glucose-derived graphite was considerably lower than yields observed from lignocellulosic precursors and were not sufficient for electrochemical performance testing of the anode material.[39] However, several studies have performed successful catalytic graphitization of glucose that produced sufficient yields for testing electrochemical performance as anode material in lithium-ion batteries. Obrovac et al. used a similar strategy to perform catalytic graphitization of glucose using an iron catalyst with a molar ratio of 87.5 : 12.5 carbon to iron.[54] Pyrolysis was carried out at 1200 °C for 3 hours. The electrochemical characteristics of the biographite were similar to synthetic graphite with a reversible capacity of 366 mAh g^{-1} and an initial coulombic efficiency of 87 % (99.7 % after 30 cycles).[54]

Several studies have employed magnesium-catalysts (as opposed to iron-catalysts) for the catalyzed graphitization of glucose. Zhao et al. generated highly graphitic carbon from glucose by first synthesizing disordered carbon at a temperature of 1000 °C for 3 hours, followed by dry mixing a magnesium catalyst (1 : 1 molar ratio) before the final graphitization.[55] The graphite powder was produced at 800 °C and 1000 °C and held for 3 or 20 hours. Following heat treatment, combined acid washing and thermal evaporation effectively purified the anode material. The graphite crystallite size increased as the treatment temperature and hold time increased with L_c measurements of 18.9 nm for the 800 °C 3 hour condition and 35.4 nm and 50.8 nm for the 1000 °C 3 hour and 20 hour conditions, respectively. When used in lithium-ion half cells, the highest specific capacity was 370 mAh g^{-1} at 50 C and was observed from the 1000 °C treatment group. This group had the best coulombic efficiency which was initially 75 % and 99.5 % after 50 cycles. Carbon coating of the anode material further increased the coulombic efficiency to 99.99 % after 50 cycles.[55] Catalytic graphitization of glucose using a magnesium catalyst was further investigated by Zhao et al. under varying conditions, from which they observed a unique, Voronoi-tessellated structure wherein graphite crystals grew outward from spheroidal graphite shells.[56] Zhao et al. produced the Voronoi-tessellated morphological graphitic carbon by conducting magnesium-catalyzed graphitization of glucose-derived disordered carbon at 800–1000 °C (Figure 10).[56] The catalyst was loaded at a ratio of 1 : 1 carbon to magnesium

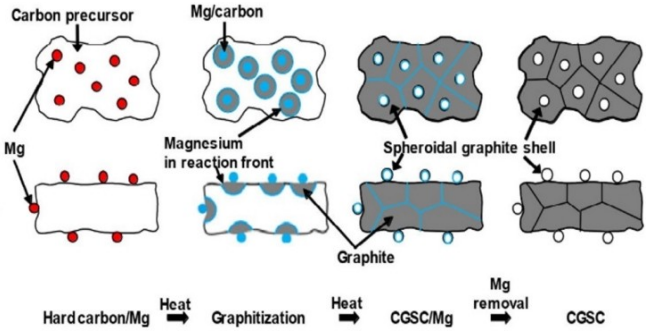

Figure 10. Voronoi-tessellated structure formation shown from an above view (top row) and cross-sectional view (bottom row).[56] Reproduced from ref. [56] Copyright (2017), with permission from Wiley-VCH.

and the maximum graphitization temperature was held for 1 or 3 hours. Graphite crystallite size increased with temperature and hold time from 185.5 nm at 800 °C and 1 hour to 222.4 nm at 1000 °C and 3 hours. Only the 1000 °C for 3 hour graphite was used for electrochemical performance analysis and a relatively low reversible capacity of 250 mAh g^{-1} was reported.[56]

Published studies focused on catalytic graphitization of carbohydrates have helped advance the field of biocarbon graphitization through an enhanced understanding of catalytic mechanisms and optimal conditions for graphitization. Glucose and sucrose are the primary carbohydrates used in published studies, and thus future work should explore other carbohydrates, including hemicellulose-derived xylose.

3.3. Catalytic Graphitization of Lignin Feedstocks

Lignin is a heterogeneous, cross-linked biopolymer with a complex chemical structure of the phenylpropane basic unit. The monomeric units are connected to each other through ether bonds and carbon-carbon linkages.[57] The structure and properties of lignin vary widely depending on the feedstock and method of isolation. Pulp, paper, and bio-ethanol industries generate significant quantities of lignin as a by-product.[58] Most of the lignin from the pulp and paper industries is used as burning fuel for steam generation. Other commercial applications of lignin include adhesives, reinforcing agents, and concrete admixtures, to name a few.[58] However, there is still a large supply of unused lignin which implies that lignin is not extensively utilized as a value-added material. The complex and inconsistent chemical structure of lignin makes it difficult to produce valuable materials from. The polyaromatic backbone of lignin makes it an attractive precursor for the production of aromatic carbon materials including carbon fibers, electrodes, and other graphitic materials.[22,49–51] Notably, lignin carbon fibers have been researched for decades and have yet to significantly penetrate the carbon fiber market, due largely to high costs and inferior strength properties.[21] Recently, researchers have explored methods to convert lignin into graphite anode

materials for lithium-ion batteries. Sagues et al. assessed three different forms of lignin as graphite precursors in their iron-catalyzed process, namely organosolv lignin, hydrolysis lignin, and kraft lignin.[39] The lignin materials were mixed with 30 wt% iron catalyst prior to graphitization at 1200 °C (10 °C min^{-1} heating rate) with a hold time of 1 hour. Kraft lignin was unable to be graphitized due to reasons that were unclear, but the presence of an appreciable amount of sulfur (1.3 wt%) likely led to iron-sulfur interactions that deteriorated the efficiency of the catalyst. In addition to catalyst poisoning, high bond dissociation energy could have caused the poor graphitization of the kraft lignin. The organosolv and hydrolysis lignins were successfully converted to biographite, albeit of lesser quality and smaller crystallite size than lignocellulose and carbohydrate precursors. The graphitic structure formed by these lignin materials had a uniform distribution that was attributed to lignin melting to a liquid intermediate phase upon heating, ensuring complete contact with the catalyst. Interestingly, the lignin precursors provide higher mass yields of the graphite product relative to other biocarbon precursors, but of lower quality and with smaller graphite crystallites.[39] Sagues et al. did not perform electrochemical performance testing using their lignin-derived graphite.

Chemical activation, using K_2CO_3 and KOH, is an emerging technique for developing porous graphitic carbon for lithium-ion battery applications.[59] The primary mechanism involved in chemical activation of non-graphitic carbon materials, such as lignin, is the development of accessible porous structures and surface area expansion which allow for greater ion adsorption and higher charge capacities.[58–60] The type of both lignin and activator strongly control the degree of graphitization, surface area, and porosity of the final carbon. Xi et al. showed high temperature pyrolysis accelerates redox reactions between the carbon and K_2CO_3 leading to the formation of reduced potassium, which then penetrates the carbon lattice, promoting local ordering and improving degree of graphitization.[59] Therefore, the hierarchical structure resultant from potassium-catalyzed graphitization should facilitate the intercalation/de-intercalation of lithium ions when used as an anode in lithium-ion batteries. Xi et al. evaluated the effects of KOH and K_2CO_3 activators on the graphitization of enzymatic hydrolysis lignin from biorefinery residues. Activators were mixed with lignin at a ratio of 1:1 before graphitization at 900 °C (heating of 10 °C min^{-1}) for 2 hours. The porous structure of the resulting graphite was significantly improved when activated by K_2CO_3, attributed to the similar transition temperatures of lignin and K_2CO_3. The biographite showed promise for lithium-ion battery applications with reversible capacities of 520 mAh g^{-1} after 200 cycles at a current density of 200 mA g^{-1} and 260 mAh g^{-1} over 1000 cycles at 1 A g^{-1}. The initial coulombic efficiency of the anode material was 74.3%. Xi et al. explored further the effects of K_2CO_3 activation on the graphitization of lignin.[61] Activator was mixed at a 1:1 ratio with softwood alkali lignin, hardwood alkali lignin, wheat alkali lignin, and enzymatic hydrolysis lignin and graphitized at 900 °C (10 °C min^{-1} heating rate) for one hour. It was determined that higher molecular weight and lower O/C ratio led to higher degrees of graphitization and porosity which ultimately led to better electrochemical performance. The highest reversible capacity of 490 mAh g^{-1} after 200 cycles at 200 mA g^{-1} was observed from the enzymatic hydrolysis lignin. The biographite from enzymatic hydrolysis lignin supported a capacity retention of 92.2% and a coulombic efficiency of 99% after 500 cycles.[61] An alternative to potassium-based chemical activators, zinc chloride showed potential in a study conducted by Li et al. where $ZnCl_2$ was used as an activator to transform lignin derived from rice husk waste into porous carbon.[58] The carbon precursor and activator were mixed at a mass ratio or 1:2 and carbonization was carried out at 500–700 °C. XRD analysis revealed that no graphitic structures were developed in the porous carbon, likely due to the low carbonization temperature. The porosity (micropores, mesopores) in the carbon structure helped demonstrate excellent electrochemical performance in terms of specific capacity (469 mAh g^{-1} after 100 cycles from 500 °C treatment). The anode material displayed a low initial coulombic efficiency of 33.3%, which was attributed to thickening of the solid electrolyte interphase (SEI) film.[58]

A non-catalytic and non-activated route has also been developed to produce graphite from lignin. Tenhaeff et al. transformed lignin into low-cost lithium-ion anode material via graphitization at the high temperatures of 1000, 1500, and 2000 °C with heating and cooling rates of 3 °C min^{-1}.[62] Average graphitic crystallite sizes were 0.9, 1.2, and 1.4 nm from the three temperatures in ascending order. The microstructure of the three graphite types were described as disordered nanocrystalline. Electrochemical performance analysis reported the highest specific capacity of 350 mAh g^{-1} after 70 cycles at 15 mA g^{-1} from the 1000 °C slurry-coated treatment group and 99.9% final coulombic efficiency. All three anode materials had >90% retention efficiency after 70 cycles at 360 mA g^{-1} with the highest from the 2000 °C type which retained 99% capacity.[62]

An increasing number of recent studies on lignin graphitization indicate that lignin is a potential precursor for lithium-ion anode materials. The motivation for using lignin as a precursor for graphite besides its high carbon content and molecular weight, is that it is also a renewable, low-cost resource and can be obtained as biomass pulping waste. However, the majority of the available lignin is from the kraft pulping process wherein the presence of inorganics (Na, S) could deactivate graphitization catalysts. Most of the aforementioned successful studies used lignin isolated by other means, such as enzyme hydrolysis, soda pulping, and organosolv pulping. Although the porous carbon materials produced from some of these lignin feedstocks have exhibited high reversible capacities, the poor initial coulombic efficiencies reported in such studies indicate structural defects in the resulting anode material. To date, little knowledge has been developed on how exactly the presence of inorganics affect the graphitization process. Therefore, more research is warranted to clarify assumptions in this area. Another potential barrier for the commercial preparation of

graphite from lignin is the lack of similarity in chemical structure from different lignin sources, which could lead to challenges associated with quality control and standardization of processes.

3.4. Catalytic Graphitization of Other Bioresources

Nonconventional biocarbon resources have also shown potential as precursors for biographite anodes in lithium-ion batteries. Boonprachai et al. evaluated the use of four different catalysts (potassium hydroxide, zinc chloride, iron (III) chloride, and magnesium) for catalytic graphitization of popped rice, which is a highly-available processed grain.[63] Carbonized popped rice samples were mixed with the four catalysts 1:2 wt% carbon to catalyst before graphitization at 800 °C (5 °C min^{-1} heating rate) with a hold time of 3 hours. The potassium hydroxide catalyzed graphite-containing carbon material had the best performance in lithium-ion battery cell testing with a specific capacity of 383 mAh g^{-1} after 100 cycles at 100 mA g^{-1}, which was much higher than the control (non-catalyzed) graphite sample which supported a reversible capacity of 189 mAh g^{-1} at the same cycling conditions.[63] While rice is a widely available crop, production of energy storage materials from the starchy grain would be in competition with food industries that rely heavily on rice. Using alternative, waste materials that need transformation to value-added products is a preferred method for graphite-precursor selection. Utilization of waste materials for developing value-added products offers opportunities for sustainable and economical reuse and circularity. Perhaps the most obvious waste material for catalytic graphitization is spent graphite recovered from lithium-ion batteries. Chen et al. developed a method to restore spent graphite via heat treatment, acid washing for purification, and cobalt salt catalyzed graphitization.[64] The spent graphite was mixed with $Co(NO3)_2$ at a ratio of 1:0.3 graphite to cobalt before restorative graphitization was performed at 900 °C for 4 hours. Initial electrochemical performance analysis of the spent anode material displayed a maximum discharge capacity of 301 mAh g^{-1} at 0.1 C and a reversible capacity of 79.5 mAh g^{-1} after 500 cycles at 1 C with an initial coulombic efficiency of 81.1%. The regenerated graphite displayed a maximum discharge capacity of 358 mAh g^{-1} in the first cycle at 0.1 C and reversible capacity of 246 mAh g^{-1} after 500 cycles at 1 C with an initial coulombic efficiency of 79.4%. Thus, the regenerated graphite anode material showed significantly higher capacity, but slightly lower initial coulombic efficiency. This approach shows the potential to decrease waste outputs and increase circularity in the field of energy storage.[64] Another, possibly more obscure feedstock for graphite-production is human hair waste. Zhu et al. designed a process for the rapid formation of graphitic porous carbon microtubes embedded with heteroatoms (O, N, S) from human hair waste via a nickel catalyst $Ni(NO3)_2$.[65] 0.6 g of clean hair was wet mixed with 0.25 g nickel catalyst and 0.5 g hexamethylenetetramine before graphitization at 650 °C (10 °C min^{-1} heating rate) for 3 hours. Impressive electrochemical performance in lithium-ion batteries (reversible capacity of 387 mAh g^{-1} at 6 Ag^{-1}, 68.5% initial coulombic efficiency, and 99.5% coulombic efficiency at the 5th cycle) implies profitable recycling potential of human hair biowaste.[65] Li et al. used chitosan, a biopolymer byproduct derived from shellfish processing, to produce a graphitic carbon@Fe3 C composite for use as lithium-ion battery anode material.[44] The feedstock chitosan was wet-mixed with $Fe(NO_3)_3$ at loading rates of 30–54 wt% before pyrolysis at 700, 800, and 900 °C (heating rate of 2 °C min^{-1}) for 2 hours. XRD analysis revealed broad (002) reflections indicating poor graphite crystal formation. The composite produced at 900 °C with 54% iron carbide demonstrated the highest reversible capacity of 423 mAh g^{-1} at 0.1 Ag^{-1} over 100 cycles with an 85% capacity retention efficiency from the first to 200th cycle. The coulombic efficiency of the half cells was initially 45% and neared 100% in subsequent cycles.[44] Thus, the relatively disordered biocarbon anode material exhibited impressive capacity, but relatively poor initial coulombic efficiency and capacity retention. In addition to marine shellfish-derived chitosan, algae-derived polymers are also an intriguing alternative feedstock for graphite synthesis. Ouyang et al. transformed porphyra (red algae) into lithium-ion anode material via catalytic graphitization with a nickel catalyst.[45] Porphyra was initially carbonized for 1 hour at 300 °C before being immersed in a 10 wt% $Ni(NO_3)_2$ solution, treated at 800 °C for 2 hours and steam activated for 1 hour at 800 °C. It was noted that the high protein content of the porphyra led to the formation of a nitrogen-doped carbon structure. Additionally, the uniform distribution of metal ions within the carbon structure was achieved via the chelation of metal ions with highly available polysaccharides in the porphyra composition. The degree of nitrogen-doping was 5.3%. The anode material had excellent electrochemical performance with reversible capacities of 1006 mAh g^{-1} at 0.1 Ag^{-1}, 278 mAh g^{-1} at 5 Ag^{-1}, and 520 mAh g^{-1} at 1 Ag^{-1} after 500 cycles. The capacity retention from the 20th to 500th cycle was 92.3% and the coulombic efficiency increased from an initial value of 66.5% to 98.7% after 200 cycles.[45]

Pyrolysis-derived heavy bio-oil is an emerging precursor for catalytic graphitization. The fast pyrolysis of woody biomass generates three types of products: bio-oil (liquid), biogas (syngas), and biochar (solid). Bio-oil contains more than 300 oxygenated compounds including alcohol, phenol, ester, aldehyde, ketone, organic acids, furans, and anhydrosugars, the majority of which are of relatively low molecular weight.[66] In addition, bio-oil consists of numerous polycyclic carbon compounds and aromatic hydrocarbons, the majority of which are relatively high molecular weight. The separation of low and high molecular weight fractions provides an opportunity for graphitization. Specifically, the low molecular weight fraction could be used for fuel and chemical synthesis, while the high molecular weight fraction could be used for graphite synthesis; this approach is similar to synthetic graphite production from high molecular weight petroleum. Due to its high carbon content, good thermo-plasticity, and low ash content, heavy bio-oil could be used as an excellent precursor for carbon electrodes. This area is relatively unexplored with few reported studies, most focused on sodium-ion battery applications as

opposed to lithium-ion batteries.[67,68] Muruganantham et al. converted bio-oil derived from rubber wood sawdust into a hard carbon material with graphitic crystallites using a ZnO template for use as anode material for sodium ion batteries.[67] Bio-oil and template were heated to 350 °C at 14 °C min^{-1} and held for one hour, then heated to 900 °C at 8 °C min^{-1} and held for one hour for complete graphitization. Electrochemical performance evaluation of half-cell sodium-ion batteries showed a reversible capacity of 198 mAh g^{-1} over 300 cycles at 100 mA g^{-1} with 99% coulombic efficiency over 500 cycles.[67] Qin et al. produced antimony-impregnated carbon nanosheets from bio-oil using an antimony chloride and sodium chloride template for sodium-ion storage applications.[68] Dried bio-oil (1 g) was wet mixed with antimony chloride (3 g) and the sodium chloride template (5 g) before the mixture was treated at 650 °C for one hour (heating rate 2 °C min^{-1}). The graphitic crystallite size obtained was 35 nm. Electrochemical performance testing in sodium-ion coin cells resulted in a reversible capacity of 391 mAh g^{-1} after 500 cycles at 1 Ag^{-1} with a retention efficiency of 90.2% compared to the fifth cycle. Coulombic efficiency was initially 54%, 98% in the third through fifth cycles, and 99% in subsequent cycles.[68] Future research on bio-oil graphitization should consider the effects of bio-oil molecular weight, bio-oil aromatic carbon content, various catalyst parameters (including particle size, surface area, porosity, oxidation state), and graphitization temperature on the electrochemical performance of developed graphitic carbon in lithium-ion batteries.

4. Catalyst Recovery

Catalytic graphitization of biomass leads to the formation of graphitic carbon structures loaded with residual metal catalyst. To purify biographite, it is therefore necessary to separate the residual catalyst from the graphitic carbon. To date, washing with strong mineral acids has been the most common method for graphite purification.[39,23,42,45,69] For example, hydrochloric acid converts iron into soluble iron chloride with the coproduction of hydrogen.

$$Fe + 2\ HCl \rightarrow FeCl_2 + H_2$$

Ferrous chloride is a valuable industrial salt and hydrogen is considered a clean fuel. Therefore, recovering ferrous chloride and capturing hydrogen would make the process economically attractive. One of the major challenges for capturing hydrogen from this reaction is the high volatility of hydrogen chloride and consequent mixing with hydrogen. However, hydrogen is non-condensable while hydrogen chloride is condensable. Therefore, an efficient condensing system can help isolate the hydrogen chloride from the mixture. The recovery of these valuable chemicals has not yet been performed in reported studies. Also, the use of strong mineral acids for removing such large amounts of catalyst may be uneconomical. Thus, more research into the techno-economic feasibility of using strong acids is needed. Several studies have explored methods that avoid or reduce the use of mineral acids. Zhao et al. used vacuum heating method to remove magnesium catalyst after graphitization.[70] Microwave digestion was also used along with acid washing to accelerate the catalyst removal.[23] Seeing that iron appears to be an effective graphitization catalyst, magnetic separation could be applied. However, a negative aspect of magnetic separation would be the efficiency of separation because the iron catalyst is strongly encapsulated by graphitic carbon. Therefore, the iron-graphite mixture would have to be thoroughly crushed before the application of a magnetic field. Magnetic separation followed by washing with a dilute acid could replace the use of concentrated mineral acids for graphite purification. Such a pathway may also enable catalyst reuse, which is another topic that has not been sufficiently addressed in the literature to date. As the field of biomass graphitization matures, optimal paths for catalyst removal and resuse should be identified.

5. Conclusions

Biographite and related biocarbon materials show promising potential to be drop-in replacements to current graphite anode materials. Current key differences preventing this replacement are lower initial coulombic efficiencies and lack of studies investigating long-term cycling performance and the specific roles feedstock contaminants play in the electrochemical performance. Nonetheless, studies show that some biomass-derived graphitic materials have excellent electrochemical performance under particular circumstances. For example, the majority of high performing materials require a catalyst and/or activator during high temperature (>1000 °C) treatment followed by catalyst/activator removal prior to cell assembly. A wide variety of biomass feedstocks have successfully produced high performing anode materials, thereby indicating that feedstock chemistry is not a limiting factor. Alternatively, the performance of anode materials (e.g. initial coulombic efficiency and capacity retention) could be improved by modifying the catalytic graphitization process to maximize catalyst-substrate interaction via reduced catalyst particle size, advanced mixing techniques, and optimal graphitization conditions for the chosen catalyst. Biomass-derived anode materials have exhibited reversible capacities that exceed the theoretical limit of graphite (~372 mAh g^{-1}), thereby indicating mechanisms other than graphite intercalation, such as lithium-ion packing within very porous or high surface area regions.[48] However, such materials typically have poor initial coulombic efficiency (<90%) and/or low capacity retention (>1% of 100 cycles), which represent barriers to commercial application. To overcome these barriers, increasing the extent of graphitization should increase stability, increase initial coulombic efficiency, and minimize capacity loses.[10] Generally, further steps that mimic the downstream processing steps used in commercial battery-grade graphite production (e.g. purification, milling, shaping, and coating) should be taken to improve thermal stability, increase initial coulombic efficiency, and minimize capacity losses.[10] Overall, there are an insufficient number of

published studies on biomass-derived anodes that include electrochemical performance data. Future studies should rely less on standard carbon material characterization techniques (XRD, Raman, BET, and SEM/TEM), and more on electrochemical testing techniques (galvanostatic charge/discharge) to achieve capacities of $>350\,mAh\,g^{-1}$ with less than 1% loss over 100 cycles and initial coulombic efficiencies $>90\%$. Lastly, efforts towards commercialization must include modifactions in process parameters to improve techno-economic viability, such as minimized catalyst loading and efficient catalyst recycling.

Acknowledgements

This research was financially supported by the Department of Energy (Award No: DE-EE0009260). The authors also acknowledge "The Nuon Project" (thenounproject.com) for the icons used in the graphical abstract. This work was authored in part by Alliance for Sustainable Energy, LLC, the manager and operator of the National Renewable Energy Laboratory (NREL) for the U.S. Department of Energy (DOE) under Contract DE-AC36-08GO28308. The views expressed in the article do not necessarily represent the views of the DOE or the U.S. Government.

Conflict of Interests

The authors declare no conflict of interest.

Data Availability Statement

The data that support the findings of this study are available from the corresponding author upon reasonable request.

Keywords: biomass · catalysis · graphite · anode · lithium-ion

[1] K. Vanstone, *Benchmark Miner. Intell.* **2019**, 2030, https://investingnews.com/daily/resource-investing/battery-metals-investing/graphite-investing/graphite-becoming-an-essential-element-in-lithium-ion-batteries/.
[2] M. Burton, E. Van Der Walt, *Bloomberg* **2017**, http://www.bloomberg.com/news/articles/2017-08-02/electric-car-revolution-is-shaking-up-the-biggest-metals-markets.
[3] D. Bogdanov, J. Farfan, K. Sadovskaia, A. Aghahosseini, M. Child, A. Gulagi, A. S. Oyewo, L. de Souza Noel Simas Barbosa, C. Breyer, *Nat. Commun.* **2019**, *10*, 1–16.
[4] E. A. Olivetti, G. Ceder, G. G. Gaustad, X. Fu, *Joule* **2017**, *1*, 229–243.
[5] G. Crabtree, *Science* **2019**, *366*, 422–424.
[6] L. Wood, *Businesswire* **2020**, http://www.businesswire.com/news/home/20200720005363/en/Lithium-ion-Battery-Market-Worth-129-Billion-by-2027-Breakdown-by-Component-End-use-Industry-and-Region-ResearchAndMarkets.com.
[7] S. Natarajan, V. Aravindan, *Adv. Energy Mater.* **2020**, *10*, 1–8.
[8] J. Zhang, C. Liang, J. B. Dunn, *Environ. Sci. Technol.* **2022**, *57*, 3402–3414.
[9] P. G. Bruce, B. Scrosati, J. M. Tarascon, *Angew. Chem. Int. Ed.* **2008**, *47*, 2930–2946.
[10] J. Li, C. Daniel, D. Wood, *J. Power Sources* **2011**, *196*, 2452–2460.
[11] J. B. Dunn, L. Gaines, M. Barnes, J. Sulliva M Wang, *Argonne Natl. Lab.* **2012**, *3*.
[12] "IPO Presentation: Spherical Graphite," *Graphex* **2016**.
[13] J. Whiteside, D. Finn-Foley, *Wood Mackenzie* **2019**, http://www.green-techmedia.com/articles/read/graphite-the-biggest-threat-to-batteries-green-reputation.
[14] A. D. Jara, A. Betemariam, G. Woldetinsae, J. Y. Kim, *Int. J. Min. Sci. Technol.* **2019**, *29*, 671–689.
[15] A. N. Sawarkar, A. B. Pandit, S. D. Samant, J. B. Joshi, *Can. J. Chem. Eng.* **2007**, *85*, 1–24.
[16] H. Pierson, *Noyes Publications* **1993**.
[17] D. P. Yang, Z. Li, M. Liu, X. Zhang, Y. Chen, H. Xue, E. Ye, R. Luque, *ACS Sustainable Chem. Eng.* **2019**, *7*, 4564–4585.
[18] J. S. McDonald-Wharry, M. Manley-Harris, K. L. Pickering, *Energy and Fuels* **2016**, *30*, 7811–7826.
[19] R. E. Franklin, *Proc. R. Soc.* **1951**, *209*.
[20] J. R. Dahn, T. Zheng, Y. Liu, J. S. Xue, *Science* **1995**, *270*, 590–593.
[21] W. J. Sagues, A. Jain, D. Brown, S. Aggarwal, A. Suarez, M. Kollman, S. Park, D. S. Argyropoulos, *Green Chem.* **2019**, *21*, 4253–4265.
[22] J. Asenbauer, T. Eisenmann, M. Kuenzel, A. Kazzazi, Z. Chen, D. Bresser, *Sustain. Energy Fuels* **2020**, *4*, 5387–5416.
[23] N. A. Banek, D. T. Abele, K. R. McKenzie, M. J. Wagner, *ACS Sustainable Chem. Eng.* **2018**, *6*, 13199–13207, https://pubs.acs.org/doi/10.1021/acssuschemeng.8b02799.
[24] W. Xu, C. Welty, M. R. Peterson, J. A. Read N P Stadie, *J. Electrochem. Soc.* **2022**, *169*, 010531.
[25] N. Lebedeva, F. Persio, L. Boon-Brett, *Eur. Comm. JRC Sci. Policy* **2016**.
[26] D. Olson, *U. S. Geol. Surv. Miner. Commod. Summ.* **2022**, *703*, 2021–2022.
[27] S. Schimmelpfennig, B. Glaser, *J. Environ. Qual.* **2012**, *41*, 1001–1013.
[28] F. Yang, H. Chen, J. Guo, P. Zheng, *J. Mater. Sci. Mater. Electron.* **2022**, *33*, 4862–4868.
[29] A. Nugroho, E. B. Nursanto, S. A. Pradanawati, H. S. Oktaviano, H. Nilasary, H. Nursukatmo, *Mater. Lett.* **2021**, *303*, 130557.
[30] X. Zhao, Y. Yao, A. E. George, R. A. Dunlap, M. N. Obrovac, *J. Electrochem. Soc.* **2016**, *163*, A858–A866.
[31] T. Kan, V. Strezov, T. J. Evans, *Renewable Sustainable Energy Rev.* **2016**, *57*, 1126–1140.
[32] M. Danish, T. Ahmad, *Renewable Sustainable Energy Rev.* **2018**, *87*, 1–21.
[33] J. P. Dees, W. J. Sagues, E. Woods, H. Goldstein, A. J. Simon, D. Sanchez, *Green Chem.* **2023**, *25*, 2930–2957.
[34] B. P. D. Laverty, L. J. Nicks, L. A. Walters, *U. S. Dept. of the Interior.* **1994**.
[35] C. M. Seah, S. P. Chai, A. R. Mohamed, *Carbon* **2014**, *70*, 1–21.
[36] D. M. Ştefănescu, G. Alonso, P. Larrañaga, E. de La Fuente, R. Suárez, *Mater. Sci. Forum* **2018**, *925*, 36–44.
[37] C. J. Thambiliyagodage, S. Ulrich, P. T. Araujo, M. G. Bakker, *Carbon* **2018**, *134*, 452–463.
[38] D. M. Stefanescu, R. Huff, G. Alonso, P. Larrañaga, E. De la Fuente, R. Suarez, *Metall. Mater. Trans. A* **2016**, *47*, 4012–4023.
[39] W. J. Sagues, J. Yang, N. Monroe, S. D. Han, T. Vinzant, M. Yung, H. Jameel, M. Nimlos, S. Park, *Green Chem.* **2020**, *22*, 7093–7108.
[40] A. Gomez-Martin, J. Martinez-Fernandez, M. Ruttert, A. Heckmann, M. Winter, T. Placke, J. Ramirez-Rico, *ChemSusChem* **2018**, *11*, 2776–2787.
[41] A. Gomez-Martin, J. Martinez-Fernandez, M. Ruttert, M. Winter, T. Placke, J. Ramirez-Rico, *ACS Omega* **2019**, *4*, 21446–21458.
[42] N. A. Banek, K. R. McKenzie, D. T. Abele, M. J. Wagner, *Sci. Rep.* **2022**, *12*, 1–11.
[43] M. P. Illa, C. S. Sharma, M. Khandelwal, *Mater. Today Chem.* **2021**, *20*, 100439.
[44] B. Li, Y. Zhang, J. Xiong, Y. Gui, T. Huang, J. Peng, H. Liu, F. Yang, M. Li, *J. Mater. Sci.* **2022**, *57*, 9939–9954.
[45] H. Ouyang, Q. Gong, C. Li, J. Huang, Z. Xu, *Mater. Lett.* **2019**, *235*, 111–115.
[46] F. H. Isikgor, C. R. Becer, *Polym. Chem.* **2015**, *6*, 4497–4559.
[47] S. G. Wettstein, D. Martin Alonso, E. I. Gürbüz, J. A. Dumesic, *Curr. Opin. Chem. Eng.* **2012**, *1*, 218–224.
[48] F. Destyorini, W. C. Amalia, Y. Irmawati, A. Hardiansyah, S. Priyono, F. Aulia, H. S. Oktaviano, Y.-I. Hsu, R. Yudianti, H. Uyama, *Energy Fuels* **2022**, *36*, 5444–5455.
[49] F. Wu, R. Huang, D. Mu, B. Wu, Y. Chen, *Electrochim. Acta* **2016**, *187*, 508–516.
[50] B. Gyenes, D. A. Stevens, V. L. Chevrier, J. R. Dahn, *J. Electrochem. Soc.* **2015**, *162*, A278–A283.
[51] S. V. Vassilev, D. Baxter, L. K. Andersen, C. G. Vassileva, *Fuel* **2010**, *89*, 913–933.
[52] X. Zhang, D. Kong, X. Li, L. Zhi, *Adv. Funct. Mater.* **2019**, *29*, 1806061.
[53] D. Ruan, L. Wu, F. Wang, K. Du, Z. Zhang, K. Zou, X. Wu, G. Hu, *J. Electroanal. Chem.* **2021**, *884*, 115073.

[54] M. N. Obrovac, X. Zhao, L. T. Burke, R. A. Dunlap, *Electrochem. Commun.* **2015**, *60*, 221–224.
[55] L. Zhao, J. C. Bennett, M. N. Obrovac, *Carbon* **2018** *134*, 507–518, doi: 10.1016/j.carbon.2018.03.017.
[56] L. Zhao, X. Zhao, L. T. Burke, J. C. Bennett, R. A. Dunlap, M. N. Obrovac, *ChemSusChem* **2017**, *10*, 3409–3418.
[57] F. S. Chakar, A. J. Ragauskas, *Ind. Crops Prod.* **2004**, *20*, 131–141.
[58] Y. Li, Y. Huang, K. Song, X. Wang, K. Yu, C. Liang, *ChemistrySelect* **2019**, *4*, 4178–4184.
[59] Y. Xi, Y. Wang, D. Yang, Z. Zhang, W. Liu, Q. Li, X. Qiu, *J. Alloys Compd.* **2019**, *785*, 706–714.
[60] S. E. Chun, J. F. Whitacre, *Microporous Mesoporous Mater.* **2017**, *251*, 34–41.
[61] Y. Xi, D. Yang, Y. Wang, J. Huang, M. Yan, C. Yi, Y. Qian, X. Qiu, *Holzforschung* **2020**, *74*, 293–302.
[62] W. E. Tenhaeff, O. Rios, K. More, M. A. McGuire, *Adv. Funct. Mater.* **2014**, *24*, 86–94.
[63] R. Boonprachai, T. Autthawong, O. Namsar, C. Yodbunork, W. Yodying, T. Sarakonsri, *Crystals* **2022**, *12*, 1–15.
[64] Q. Chen, L. Huang, J. Liu, Y. Luo, Y. Chen, *Carbon* **2022**, *189*, 293–304.
[65] J. Zhu, S. Liu, Y. Liu, T. Meng, L. Ma, H. Zhang, M. Kuang, J. Jiang, *ACS Sustainable Chem. Eng.* **2018**, *6*, 13662–13669.
[66] X. Hu, M. Gholizadeh, *J. Energy Chem.* **2019**, *39*, 109–143.
[67] R. Muruganantham, T. H. Hsieh, C. H. Lin, W. R. Liu, *Mater. Today Energy* **2019**, *14*, 100346.
[68] B. Qin, H. Jia, Y. Cai, M. Li, J. Qi, J. Cao, J. Feng, *J. Colloid Interface Sci.* **2021**, *582*, 459–466.
[69] A. Gutiérrez-Pardo, J. Ramírez-Rico, R. Cabezas-Rodríguez, J. Martínez-Fernández, *J. Power Sources* **2015**, *278*, 18–26.
[70] L. Zhao, X. Zhao, L. T. Burke, J. C. Bennett, R. A. Dunlap, M. N. Obrovac, *ChemSusChem* **2017**, *10*, 3409–3418.

Manuscript received: May 21, 2023
Revised manuscript received: August 28, 2023
Accepted manuscript online: August 29, 2023
Version of record online: October 10, 2023